PERGAMON

International Journal of Solids and Structures 38 (2001) 5205–5214

INTERNATIONAL JOURNAL OF SOLIDS and STRUCTURES

www.elsevier.com/locate/ijsolstr

Dynamic growth of an internal circular crack in a transversely isotropic composite

Y.M. Tsai *

Department of Aerospace Engineering and Engineering Mechanics, Iowa State University, 2271 Howe Hall, Room 1200, Ames, Iowa 50011-2271, USA

Received 8 March 2000

Abstract

The dynamic growth of an internal circular crack in a transversely isotropic composite is investigated using the techniques of Hankel and Laplace transforms. The Laplace inversion is carried out through a complete contour integration. For the crack running at a constant speed, exact dynamic solutions for crack shape and stress distribution with singularities in the crack plane are obtained in closed forms in terms of anisotropic material constants and crack speed.

Graphite/epoxy and E glass/epoxy materials and an isotropic material are used as example materials in calculating the numerical values of the dynamic stress intensity factor and crack shape. The dynamic solution reduces to the static solution at zero crack speed and deviates at speeds other than zero. Deviation between dynamic and static solutions is governed by dynamic correction factors, which are non-dimensional functions of anisotropic material constant ratios and the ratio between crack speed and shear-wave speed. Values of these dynamic factors are obtained for the sample composites for a large range of crack speed.

Keywords: Dynamic growth; Circular crack; Isotropic composite

1. Introduction

The dynamic problem of a circular crack propagating in an infinite isotropic elastic solid was investigated by Kostrov (1964). The results obtained were largely the highest order approximations in the immediate neighborhood of the crack tip. Dynamic propagation toughness was measured as a function of crack speed by means of caustics (Kalthoff et al., 1980). Study of rapid crack propagation is important in the understanding of dynamic fracture and crack arrest.

Composite materials have recently been used in many structural applications. Transversely isotropic material with five elastic constants was shown to be sufficient to characterize many fiber-reinforced composites (Christensen, 1979). For a stationary penny-shaped crack in a transversely isotropic infinite elastic solid, under static loading, the normal stress distribution in the crack plane was found to be identical with

* Tel.: +515-294-3124; fax: +515-294-3262.
E-mail address: ytsai@iastate.edu (Y.M. Tsai).

PII: S0020-7683(00)00347-4

that for the corresponding isotropic solution (Elliott, 1949). Consequently, the static stress intensity factor is the same for the isotropic and the transversely isotropic media.

The dynamic response to vibratory normal stresses in a transversely isotropic material containing an external circular crack was studied in an earlier work (Tsai, 1992). The dynamic growth of a circular crack in a transversely isotropic composite is investigated in the present work. The problem is solved using the techniques of Hankel and Laplace transforms. The Laplace inversion is carried out through a complete contour integration. For the crack running at a constant speed, exact dynamic expressions for the crack shape and the stress intensity factor are obtained in terms of anisotropic material constants and crack speed. The effects that the material anisotropy and the crack speed have on the fracture behavior are investigated for graphite/epoxy and glass/epoxy composites.

2. Transformed solution

The stress–strain relationship in cylindrical coordinates (r, θ, z) for a transversely isotropic composite can be written in the following form (Christensen, 1979):

$$\begin{aligned} \sigma_{rr} &= c_{11}e_{rr} + c_{12}e_{\theta\theta} + c_{13}e_{zz} \\ \sigma_{\theta\theta} &= c_{12}e_{rr} + c_{11}e_{\theta\theta} + c_{13}e_{zz} \\ \sigma_{zz} &= c_{13}e_{rr} + c_{13}e_{\theta\theta} + c_{33}e_{zz} \\ \sigma_{rz} &= c_{44}e_{rz} \\ \sigma_{\theta z} &= c_{44}e_{\theta z} \\ \sigma_{r\theta} &= (c_{11} - c_{12})e_{r\theta}/2 \end{aligned} \tag{1}$$

The z-axis is along the axis of symmetry of the material. An infinite transversely isotropic elastic solid is assumed to carry a uniform tension p_0 in the z-direction at infinity. A circular crack starts to propagate at time t equal to zero and has current radius $a(t)$ in a plane perpendicular to the direction of tension. Solution of the problem can be obtained by superposing a uniform tension p_0 on the stress fields set up by a uniform pressure, $-p_0$, which acts on the crack surfaces.

The wave field generated by the propagating crack is axisymmetrical and its displacement components can be described as $(u_r, 0, u_z)$. The boundary conditions on the crack plane $z = 0$ for $t > 0$ are

$$\sigma_{zr} = 0 \tag{2}$$

$$u_z = \begin{cases} w(r), & r < a \\ 0, & r > a \end{cases} \tag{3}$$

The unknown function $w(r)$ describes the crack surface and is to be determined later. Using the strain–displacement relations, the equations of motion can be written in terms of the displacement components as follows:

$$\beta \frac{\partial}{\partial r}\left[\frac{1}{r}\frac{\partial}{\partial r}(ru_r)\right] + (1+\delta)\frac{\partial^2 u_z}{\partial r \partial z} + \frac{\partial^2 u_r}{\partial z^2} = \frac{1}{c_2^2}\frac{\partial^2 u_r}{\partial t^2} \tag{4}$$

$$\frac{1}{r}\frac{\partial}{\partial r}\left(r\frac{\partial u_z}{\partial r}\right) + (1+\delta)\frac{\partial}{\partial z}\left[\frac{1}{r}\frac{\partial}{\partial r}(ru_r)\right] + \alpha\frac{\partial^2 u_z}{\partial z^2} = \frac{1}{c_2^2}\frac{\partial^2 u_z}{\partial t^2} \tag{5}$$

$$\beta = c_{11}/c_{44'}, \qquad \alpha = c_{33}/c_{44'}, \qquad \delta = c_{13}/c_{44'}, \qquad c_2 = \sqrt{c_{44}/\Delta} \tag{6}$$

The quantity Δ is the density of the medium.

The Laplace transform is operated over the time variable t in Eqs. (4) and (5) and is designated as $f^*(p)$. In addition, the first-order and zeroth-order Hankel transforms are respectively applied to Eqs. (4) and (5) over the variable r with the transform parameter s. The transformed equations have the following forms:

$$\frac{\partial^2 \overset{*}{\hat{u}}{}_r^1}{\partial z^2} - \left(s^2 + p^2/c_2^2\right)\overset{*}{\hat{u}}{}_r^1 - (1+\delta)s\frac{\partial \overset{*}{\hat{u}}{}_z^0}{\partial z} = 0 \tag{7}$$

$$\alpha\frac{\partial^2 \overset{*}{\hat{u}}{}_z^0}{\partial z^2} - \left(s^2 + p^2/c_2^2\right)\overset{*}{\hat{u}}{}_z^0 + (1+\delta)s\frac{\partial \overset{*}{\hat{u}}{}_r^1}{\partial z} = 0 \tag{8}$$

The function $\hat{u}_r^1$ is the first-order Hankel transform of u_r while $\hat{u}_z^0$ is the zeroth-order Hankel transform of u_z. To solve the problem, the transformed displacements are chosen of the following forms.

$$\overset{*}{\hat{u}}{}_r^1 = Ae^{-kz}, \qquad \overset{*}{\hat{u}}{}_z^0 = Be^{-kz} \tag{9}$$

Eqs. (7) and (8) lead to the following characteristic equation for the parameter k:

$$\left[\alpha k^2 - \left(s^2 + p^2/c_2^2\right)\right]\left[k^2 - \left(s^2 + p^2/c_2^2\right)\right] + (1+\delta)^2 s^2 k^2 = 0 \tag{10}$$

The equation can be seen as a quadratic equation for k^2 and has two roots, k_1^2 and k_2^2. The positive roots, k_1 and k_2 are used in Eq. (9) in order to satisfy the radiation conditions. A more detailed description on the properties of the roots will be presented later in connection with the Laplace inversion. Each root requires two constants in Eq. (9). The constants are related through Eq. (8) in the following forms:

$$A_i k_i s = \left[\alpha k_i^2 - \left(s^2 + p^2/c_2^2\right)\right]B_1/(1+\delta) \tag{11}$$

The subscript i has the range of 1 and 2.

The shearing stress σ_{zr} can be calculated in terms of Eqs. (1), (9) and (11). Satisfying the stress boundary condition in Eq. (2) yields

$$B_1\left(\alpha k_1^2 + \delta s^2 - p^2/c_2^2\right) = -\left(\alpha k_2^2 + \delta s^2 - p^2/c_2^2\right)B_2 \tag{12}$$

If Eqs. (9) and (12) are used, the displacement boundary condition gives

$$B_2 = \left[\alpha k_1^2 + \delta s^2 - p^2/c_2^2\right]\overset{*}{\hat{w}}{}^0/\left(k_1^2 - k_2^2\right)\alpha \tag{13}$$

$$\hat{w}^0 = \int_0^a w(r)rJ_0(sr)\mathrm{d}r \tag{14}$$

The transform of the normal stress σ_{zz} can be calculated in terms of Eqs. (1), (9) and (11)–(13). The results can be written as follows:

$$\overset{*}{\hat{\sigma}}{}_{zz}^0 = -\overset{*}{\hat{w}}{}^0\left[\Delta p^2 F_1 + c_{44}pF_2\right] \tag{15}$$

$$F_1 = \left[1 + p^2/k_1k_2c_2^2\right]/(k_1+k_2) \tag{16}$$

$$F_2 = \left[b_1 s^4 + a_1 p^2 s^2/c_2^2\right]/p(k_1+k_2)k_1k_2 \tag{17}$$

$$a_1 = 1 + \beta - \delta^2/\alpha \tag{18}$$

$$b_1 = \beta - \delta^2/\alpha \tag{19}$$

Eq. (15) is used to satisfy the condition of pressure acting on the crack surface and to solve for the unknown crack shape function $w(r)$.

3. Dynamic crack surface displacement

The Laplace inversion of Eq. (15) is carried out by treating each term on the right-hand side as a separate transform function. For the evaluation of the Laplace inversion integrals, the transformation $p = sc_2\xi$ is used in the calculations. After the transformation, the new forms of the characteristic roots can be written as

$$q_1 = k_1/s = \left\{\left[\gamma + (1+\alpha)\zeta^2 + \varphi\right]/2\alpha\right\}^{1/2} \tag{20}$$

$$q_3 = k_2/s = \left\{\left[\gamma + (1+\alpha)\zeta^2 - \varphi\right]/2\alpha\right\}^{1/2} \tag{21}$$

$$\varphi^2 = \left[\gamma + (1+\alpha)\zeta^2\right]^2 - 4\alpha\left[\zeta^4 + (1+\beta)\zeta^2 + \beta\right] \tag{22}$$

$$\gamma = 1 + \alpha\beta - (1+\delta)^2 \tag{23}$$

The roots of φ in Eq. (22) are complex for the composite materials to be considered. The roots are the branch points of q_1 and q_3 (Payton, 1983; Tsai and Kolsky, 1967; Tsai, 1992). In addition, q_1 has the branch point at $\zeta = \pm \mathrm{i}\beta^{1/2}$ and q_3 has the branch point at $\zeta = \pm\mathrm{i}$. The augmentation of two elastic constants for an isotropic material (Tsai and Kolsky, 1967; Tsai, 1971) to the five material constants for the current transversely isotropic material has greatly increased the complexity of the problem considered. The integrands of the integrals obtained in the present work are mostly different from those for the associated isotropic integral and involve four branch points instead of two branch points for an isotropic material (Tsai and Kolsky, 1967; Tsai, 1971). The infinite integrals which are obtained through the process of Laplace transform in the current problem are different from the frequency integrals for a very different set of boundary conditions involved in the earlier work (Tsai, 1992). A completely different contour involving four branch points is devised in the evaluations of the current Laplace inversion integrals. The inversion of F_1 in Eq. (16) can be written in the following form:

$$f_1 = \ell^{-1}[F_1] = c_2 L_1 \sin(sc_2\eta t) \tag{24}$$

The operator L_1 has the following form

$$\begin{aligned} L_1 f(g\eta) = {} & \frac{2}{\pi}\int_1^{\sqrt{\beta}} \alpha\left[|q_3| - \sqrt{\alpha}\eta^2 q_1\left(\beta - \eta^2\right)^{-1/2}\left(\eta^2 - 1\right)^{-1/2}\right] f(g\eta)\,\mathrm{d}\eta/\varphi \\ & + \frac{2}{\pi}\int_{\sqrt{\beta}}^{\infty}\left[1 + \sqrt{\alpha}\eta^2\left(\eta^2 - \beta\right)^{-1/2}\left(\eta^2 - 1\right)^{-1/2}\right] f(g\eta)\,\mathrm{d}\eta/(|q_1| + |q_3|) \end{aligned} \tag{25}$$

The function F_2 in Eq. (17) has a pole at $p = 0$ and its inversion results from the contributions of the pole and the branch cuts are as follows:

$$f_2 = \ell^{-1}[F_2] = s[f_0 + L_2\cos(sc_2\eta t)] \tag{26}$$

$$f_0 = b_1/\left[2\beta/\alpha + \gamma\beta^{1/2}\alpha^{-3/2}\right] \tag{27}$$

$$\begin{aligned} L_2 f(g\eta) = {} & \frac{2}{\pi}\int_1^{\sqrt{\beta}} \alpha^{3/2}\left[a_1\eta^2 - b_1\right] q_1 f(g\eta)\,\mathrm{d}\eta/\eta\varphi\left(\beta - \eta^2\right)^{1/2}\left(\eta^2 - 1\right)^{1/2} \\ & + \frac{2}{\pi}\int_{\sqrt{\beta}}^{\infty} \alpha^{1/2}\left[b_1 - a_1\eta^2\right] f(g\eta)\,\mathrm{d}\eta/\eta\left(\eta^2 - \beta\right)^{1/2}\left(\eta^2 - 1\right)^{1/2}(|q_1| + |q_3|) \end{aligned} \tag{28}$$

The material constants ratio f_0 in Eq. (27) is the contribution of the pole.

Laplace and Hankel inversions of Eq. (15) give the normal stress at $z=0$ as

$$\sigma_{zz}(r,t) = \sigma_{zz}^0 - \rho c_2 L_1 Q_1 - c_{44} L_2 Q_2 \tag{29}$$

$$\sigma_{zz}^0 = -f_0 c_{44} \int_0^\infty J_0(sr) s^2 \hat{w}^0 \,\mathrm{d}s \tag{30}$$

$$Q_1 = \int_0^\infty J_0(sr) s \frac{\partial}{\partial t} \int_0^t \sin[sc_2\eta(t-\tau)] \frac{\partial}{\partial \tau} \hat{w}^0 \,\mathrm{d}\tau \,\mathrm{d}s \tag{31}$$

$$Q_2 = \int_0^\infty J_0(sr) s^2 \int_0^t \cos[sc_2\eta(t-\tau)] \frac{\partial}{\partial \tau} \hat{w}^0 \,\mathrm{d}\tau \,\mathrm{d}s \tag{32}$$

where $J_0(x)$ is the zeroth-order Bessel function. The unknown crack shape function w in the above integrals can be solved from Eq. (29) by the successive approximation techniques similar to those used in an earlier work (Tsai, 1972). The last two terms on the right-hand side of Eq. (29) are the wave-effects terms. In the process of solution, these two terms are first dropped to form a reduced equation. The double integration techniques (Tsai, 1972) are then applied over the reduced equation to obtain the following first approximation.

$$w_1(r,t) = -\frac{2}{\pi} \frac{1}{f_0 c_{44}} \int_r^a \frac{\mathrm{d}\xi}{\sqrt{\xi^2 - r^2}} \int_0^\xi \frac{m\sigma_{zz}\,\mathrm{d}m}{\sqrt{\xi^2 - m^2}} \tag{33}$$

The normal stress σ_{zz} is equal to the pressure, $-p_0$, over the crack surface. Under this condition, the associated static crack shape function w_1 in Eq. (33) becomes

$$w_1 = \frac{2}{\pi} \frac{p_0}{f_0 c_{44}} \left(a^2 - r^2\right)^{1/2} \tag{34}$$

In terms of Eq. (34), the time derivative in the integrands in Eqs. (31) and (32) is found as

$$\frac{\partial}{\partial t} \hat{w}_1^0 = \frac{\partial}{\partial t} \int_0^a w_1 \lambda J_0(\lambda s) \,\mathrm{d}\lambda = \frac{2}{\pi} \frac{p_0}{f_0 c_{44}} \frac{\sin(sa)}{s} a\dot{a} \tag{35}$$

To obtain the second approximation, the double integrations in Eq. (33) are applied over Eq. (29). The results can be written in terms of Eq. (35) in the following form.

$$w_2 = w_1 - \left(\frac{2}{\pi}\right)^2 \frac{p_0}{f_0^2 c_{44}} \int_r^a \frac{\mathrm{d}\xi}{\sqrt{\xi^2 - r^2}} \left\{ \frac{L_1}{c_2} \frac{\partial}{\partial t} I_1 - L_2 \frac{\partial}{\partial \xi} I_2 \right\} \tag{36}$$

$$I_1 = \int_0^t \int_0^\infty \frac{\sin(\xi s)\sin[sc_2\eta(t-\tau)]\sin(sa)}{s} \mathrm{d}s\, a\dot{a}\,\mathrm{d}\tau \tag{37}$$

$$I_2 = \int_0^t \int_0^\infty \frac{\cos(\xi s)\cos[sc_2\eta(t-\tau)]\sin(sa)}{s} \mathrm{d}s\, a\dot{a}\,\mathrm{d}\tau \tag{38}$$

For a crack propagating at a constant speed of V, the quantities a and $\dot{a}$ are respectively equal to V_τ and V. The numerators in Eqs. (37) and (38) are expressed as sums of sine functions. The integrations over s can then be carried out using the following identity.

$$\int_0^\infty \frac{\sin sx}{s} \mathrm{d}s = \begin{cases} \pi/2, & x > 0 \\ -\pi/2, & x < 0 \end{cases} \tag{39}$$

For $\xi < a$, integrations over s and τ in Eqs. (37) and (38) leads to the following results:

$$\frac{\partial}{\partial t} I_1 = c_2 \frac{\pi}{2} \frac{v_2^2 \eta \xi}{(\eta + v_2)^2}, \qquad \frac{\partial}{\partial \xi} I_2 = -\frac{\pi}{2} \frac{v_2^2 \xi}{(\eta + v_2)^2} \tag{40}$$

where $v_2 = V/c_2$. Upon substituting Eq. (40) into Eq. (36), the second approximation becomes:

$$w_2 = \frac{2}{\pi} \frac{p_0}{f_0 c_{44}} \sqrt{a^2 - r^2}[1 - \epsilon] = w_1(1 - \epsilon) \tag{41}$$

$$\epsilon = \frac{v_2^2}{f_0} \left[L_1 \frac{\eta}{(\eta + v_2)^2} + L_2 \frac{1}{(\eta + v_2)^2} \right] \tag{42}$$

If all the higher order approximations are carried out in the way similar to that for w_2, the solution for $w(r)$ results in an infinite series which can be summed into a closed form as follows:

$$w = w_1 \left(1 - \epsilon + \epsilon^2 - \epsilon^3 + \cdots \right) = \frac{2p_0}{\pi K_D} \left(a^2 - r^2\right)^{1/2} \tag{43}$$

$$K_D = f_0 c_{44} (1 + \epsilon) \tag{44}$$

The dynamic correction term ϵ can be seen in Eq. (42) to be vanishing when the crack speed V tends to zero. At this limiting case, the dynamic crack surface function in Eq. (43) reduces to the corresponding static function in Eq. (34).

4. Dynamic stress intensity factor

The normal stress σ_{zz} in Eq. (29) is found to be singular at the crack tip. For $r > a$, the associated static normal stress in Eq. (30) is calculated in terms of w in Eq. (43) by using the techniques similar to those used in an earlier work (Tsai, 1972) to have the following form.

$$\sigma_{zz}^0 = \frac{2p_0}{\pi(1 + \epsilon)} \left[\frac{a}{\sqrt{r^2 - a^2}} - \sin^{-1} \frac{a}{r} \right] \tag{45}$$

To calculate the values of Q_1 and Q_2, the Abel transform is applied over r, giving

$$\overline{Q}_1 = \int_0^{\xi} \frac{m Q_1 \mathrm{d}m}{\sqrt{\xi^2 - m^2}} = \frac{2p_0}{\pi K_D} \frac{\partial}{\partial t} I_1 \tag{46}$$

$$\overline{Q}_2 = -\frac{2p_0}{\pi K_D} \frac{\partial}{\partial \xi} I_2 \tag{47}$$

The dynamic crack shape function w in Eq. (43) is used in the above calculations. For $r < a$, the integrated expressions for $\partial I_1/\partial t$ and $\partial I_2/\partial \xi$ are given in Eq. (40). Similar techniques of integrations are used for $a < r < c_2 \eta t$ and the results are

$$\frac{\partial}{\partial t} I_1 = c_2 \pi v_2^2 \eta^2 (\eta a - v_2 \xi) / \left(\eta^2 - v_2^2\right)^2 \tag{48}$$

$$\frac{\partial}{\partial \xi} I_2 = \pi v_2^2 \eta \left(\eta a - v_2^2 \xi\right) / \left(\eta^2 - v_2^2\right)^2 \tag{49}$$

The inverse Abel transform of Eq. (46) recovers the function

$$Q_1 = \frac{2}{\pi}\frac{1}{r}\frac{\mathrm{d}}{\mathrm{d}r}\int_0^r \frac{\xi}{\left(r^2-\xi^2\right)^{1/2}}\left[\frac{2}{\pi}\frac{p_0}{K_{\mathrm{D}}}\frac{\partial}{\partial t}I_1\right]\mathrm{d}\xi \tag{50}$$

The same inverse transform of Eq. (47) gives Q_2.

The functions Q_1 and Q_2, after integrations, are substituted, together with Eq. (45), into Eq. (29) to obtain the following dynamic normal stress

$$\sigma_{zz} = \frac{2p_0}{\pi}\left\{G_1\frac{a}{\sqrt{r^2-a^2}} - G_2\sin^{-1}\frac{a}{r} + G_3\right\} \tag{51}$$

$$(1+\epsilon)G_1 = 1 + \frac{v_2^2}{f_0}\left\{L_1\left[\frac{\eta}{(\eta+v_2)^2} - \frac{2\eta^2(\eta-v_2)}{(\eta^2-v_2^2)^2}\right] + L_2\left[\frac{1}{(\eta+v_2)^2} - \frac{2\eta(\eta-v_2)}{(\eta^2-v_2^2)^2}\right]\right\} \tag{52}$$

$$(1+\epsilon)G_2 = 1 + \frac{v_2^2}{f_0}\left\{L_1\left[\frac{\eta}{(\eta+v_2)^2} + \frac{2v_2\eta^2}{(\eta^2-v_2^2)^2}\right] + L_2\left[\frac{1}{(\eta+v_2)^2} + \frac{2v_2\eta}{(\eta^2-v_2^2)^2}\right]\right\} \tag{53}$$

$$(1+\epsilon)G_3 = \frac{\pi v_2^3}{f_0}\left[L_1\frac{\eta^2}{(\eta^2-v_2^2)^2} + L_2\frac{\eta}{(\eta^2-v_2^2)^2}\right] \tag{54}$$

The first term on the right-hand side of Eq. (51) is a singular term. The dynamic stress intensity factor is calculated from this singular term as

$$K_{\mathrm{ID}} = G_1K_{\mathrm{I}}; \qquad K_{\mathrm{I}} = 2p_0(a/\pi)^{1/2} \tag{55}$$

The dynamic stress intensity factor K_{ID} is found above as the product of the static stress intensity factor K_{I} and the dynamic correction factor G_1.

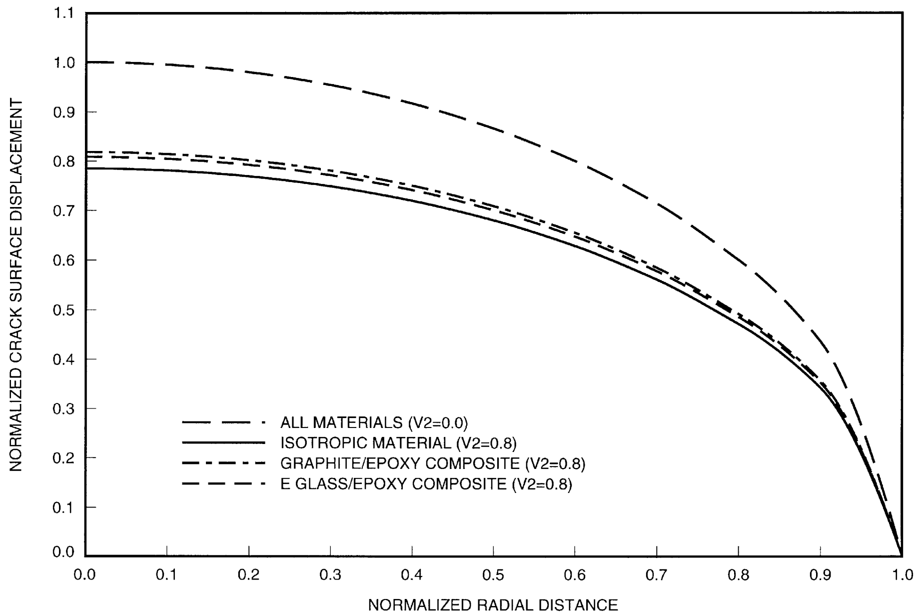

Fig. 1. Normalized crack surface opening $w/(2ap_0/\pi f_0 c_{44})$ as a function of the normalized radial distance, r/a.

For an isotropic material, the elastic constants are $c_{11} = c_{33} = \lambda + 2\mu$, $c_{12} = c_{13} = \lambda$ and $c_{44} = \mu$, where λ and μ are the Lame constants. For these constants, the quantity f_0 in Eq. (27) becomes $1/(1 - v)$, v being Poisson's ratio. For an isotropic material at zero crack speed, the crack surface function in Eq. (43) and the normal stress distribution in Eq. (51) reduce to the corresponding results given by Sneddon (1951).

Graphite/epoxy composite has been described as a transversely isotropic material (Rose et al., 1988) and the five material constants are $c_{11} = 14.5$, $c_{33} = 139$, $c_{13} = 3.75$, $c_{12} = 8.08$ and $c_{44} = 5.33$, all in the units of GPa. E glass/epoxy composite is also a transversely isotropic material (Behrens, 1971) and has the anisotropic elastic constants in GPa as $c_{11} = 14.93$, $c_{33} = 47.27$, $c_{13} = 5.244$, $c_{12} = 6.567$ and $c_{44} = 4.745$. These two materials are used as sample materials for calculations to study anisotropy and crack speed effects. For comparison, polycrystalline magnesium with Young's modulus $E = 4.1 \times 10^6$ N/cm^2 and Poisson's ratio $v = 0.3$ (Elliott, 1949) is also used here as an example isotropic material.

The dynamic crack surface displacement w is calculated from Eq. (43) for the sample materials at various crack speeds. The results are normalized by the associated maximum static crack opening $2ap_0/\pi f_0 c_{44}$. Typical normalized crack openings are shown in Fig. 1 for $v_2 = 0$ and $v_2 = 0.8$. The normalized crack surface displacement at the center of the crack is shown in Fig. 2 as a function of the normalized crack speed for the sample materials. The dynamic stress intensity factor is also calculated from Eq. (55). The values normalized by the associated static stress intensity factor are shown in Fig. 3 for a wide range of the crack speed.

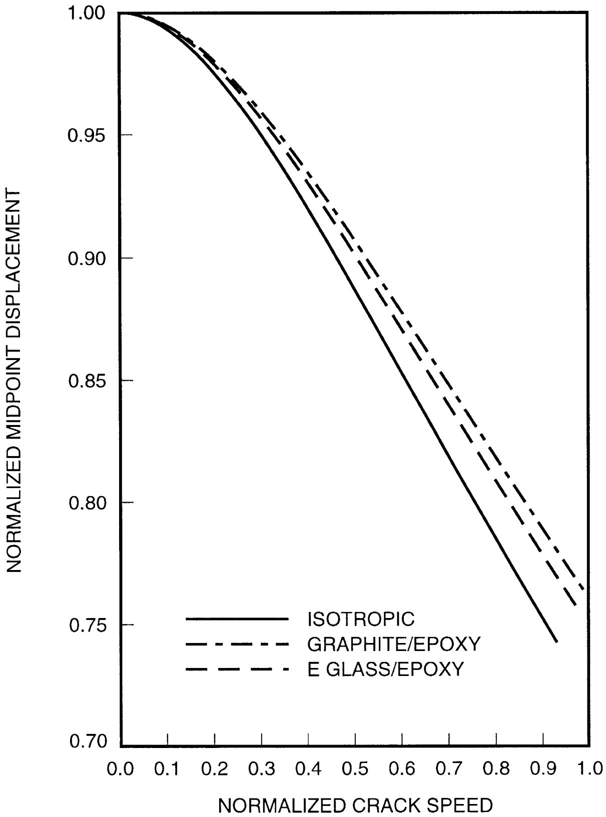

Fig. 2. Normalized crack center displacement $w(0)/(2ap_0/\pi f_0 c_{44})$ as a function of the normalized crack speed $v_2 = V/c_2$.

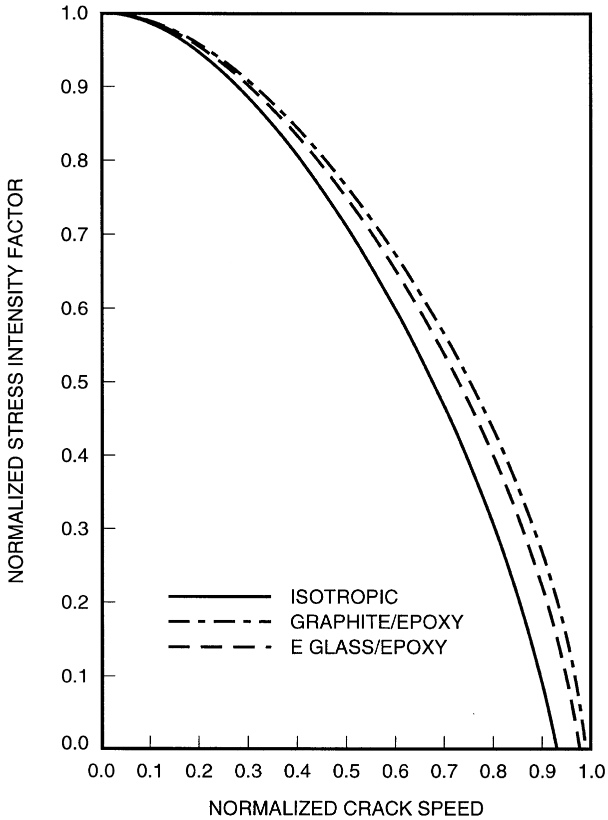

Fig. 3. Normalized dynamic stress intensity factor $K_{\mathrm{ID}}/K_{\mathrm{I}}$ as a function of the normalized crack speed $v_2 = V/c_2$.

5. Conclusion

An internal circular crack propagating in a transversely isotropic composite is investigated using the techniques of Hankel and Laplace transforms. The Laplace inversion integral is evaluated through a complete contour integration. For the crack running at a constant speed, exact dynamic solutions for the crack shape and the normal stress distribution with singularities in the crack plane are obtained in closed forms in terms of anisotropic material constants and crack speed. The dynamic solution reduces to the associated static solution at zero crack speed. When the crack propagates, the deviation of the dynamic solution from the static solution is governed by dynamic correction factors which are nondimensional functions of the ratios among anisotropic material constants and the ratio of the crack speed to the shear-wave speed.

The dynamic crack surface opening and stress intensity factor are calculated numerically for graphite/epoxy and E glass/epoxy composite materials and an isotropic material for a large range of crack speed. The dynamic crack surface openings for both composite and isotropic material are seen in Fig. 1 to be less than the corresponding static opening. The crack surface displacement at the center of the crack in the composites are shown in Fig. 2 to be larger than the corresponding isotropic crack surface displacement at various crack speeds. The dynamic stress intensity factors for the composites are also seen in Fig. 3 to be higher than the dynamic isotropic values for a large range of crack speed. Because of different degrees of anisotropy, the dynamic crack surface opening and stress intensity factor for the graphite/epoxy composite are shown in Figs. 1–3 to be higher than the corresponding values for the E glass/epoxy composite.

References

Behrens, E., 1971. Elastic constants of fiber-reinforced composite with transversely isotropic constituents. J. Appl. Mech. 38, 1062–1065.

Christensen, R.M., 1979. Mechanics of Composite Materials. Wiley, New York, p. 140.

Elliott, H.A., 1949. Axial symmetric stress distributions in aeolotropic hexagonal crystals. The problem of the plane and related problems, Proceedings of the Camb. Phil. Soc., vol. 44. pp. 522–533.

Kalthoff, J.F., Beinart, J., Winkler, S., Klemm, W., 1980. Experimental analysis of dynamic effects in different crack arrest test specimens. ASTM STP 711, Amer. Soc. for Testing and Mater., Philadelphia, PA, pp. 109–127.

Kostrov, 1964. The axisymmetric problem of propagation of a tension crack. Prikl. Mat. i Mek. 28, 793–803.

Payton, R.G., 1983. Elastic Wave Propagation in Transversely Isotropic Media. Martinus Nijhoff, The Hauge, The Netherlands, p. 136.

Rose, J.L., Pilarski, A., Balasubramaniam, K., Tverdokhlebov, A., Ditri, J. 1998. Elements of an Ultrasonic Feature Matrix NDE Technique Based on Bulk Waves and Anisotropic Elasticity. ASME, New York, vol. MD-9, pp. 63–71.

Sneddon, I.N., 1951. Fourier Transforms. McGraw-Hill, New York, p. 490.

Tsai, Y.M., Kolsky, H., 1967. A study of the fractures produced in glass blocks by impact. J. Mech. Phys. Solids 15, 263–278.

Tsai, Y.M., 1971. Dynamic contact stresses produced by the impact of an axisymmetrical projectile on an elastic half-space. Int. J. Solids Struct. 7, 543–558.

Tsai, Y.M., 1972. Stress distribution, crack shape and energy for a penny-shaped crack in a plate of finite thickness. Engng. Frac. Mech. 4, 155–169.

Tsai, Y.M., 1992. Dynamic response to normal stresses in a transversely isotropic material containing an external circular crack. J. Engng. Mater. Technol. 114 (2), 208–212.